

2

**NASA Contractor Report 187532**  
**ICASE Report No. 91-23**

**AD-A233 478**

# ICASE

**TURBULENT SEPARATED FLOW PAST A BACKWARD-  
FACING STEP: A CRITICAL EVALUATION OF  
TWO-EQUATION TURBULENCE MODELS**

**S. Thangam**  
**C. G. Speziale**

**DTIC**  
ELECTE  
APR 2 1991

**D**

**Contract No. NAS1-18605**  
**February 1991**

**Institute for Computer Applications in Science and Engineering**  
**NASA Langley Research Center**  
**Hampton, Virginia 23665-5225**

**Operated by the Universities Space Research Association**

**NASA**

**National Aeronautics and  
Space Administration**

**Langley Research Center**  
**Hampton, Virginia 23665-5225**

187532

91 4 11 004

187532-1

STEP:		1961	
MODELS		1961	<input checked="" type="checkbox"/>
			<input type="checkbox"/>
			<input type="checkbox"/>
Justification			
By			
Distribution			
Availability			
Dist	Special		
A-1	1		

**Hampton, Virginia 23665-5225**

Dist	Avail and/or Special
A-1	

‡ This research was supported by the National Aeronautics and Space Administration under NASA Contract No. NAS1-18605 while the authors were in residence at the Institute for Computer Applications in Science and Engineering (ICASE), NASA Langley Research Center, Hampton, VA 23665.

## 1. INTRODUCTION

Turbulent flow past a backward-facing step has played a central role in benchmarking the performance of turbulence models for separated flows. During the past decade — beginning with the 1980/81 Stanford conference on complex turbulent flows<sup>1</sup> — a variety of two-equation turbulence models were tested and compared with the experimental data of Kim, Kline and Johnston<sup>2</sup> and Eaton and Johnston<sup>3</sup> for the backstep problem. Initial results<sup>1</sup> indicated that the standard  $K$ - $\epsilon$  model, with wall functions, underpredicted the reattachment point by a substantial amount of the order of 20-25%. A significant number of studies have been subsequently published using alternative forms of the  $K$ - $\epsilon$  model wherein a variety of conflicting results have been reported. For example, Sindir<sup>4</sup> made modifications to account for streamline curvature based on the algebraic stress model of Gibson<sup>5</sup>; some improvements were obtained although the results were somewhat mixed. Chen<sup>6</sup> performed calculations with a multiple scale  $K$ - $\epsilon$  model wherein the turbulent kinetic energy  $K$  and the turbulent dissipation rate  $\epsilon$  were decomposed into low and high wavenumber parts along the lines suggested by Hanjalic *et al.*<sup>7</sup> Significantly improved results for the reattachment point were obtained (the underprediction was reduced to 5%), however, no detailed comparison of the Reynolds stresses were made. Speziale<sup>8</sup> reported comparable improvements for the backstep problem based on an anisotropic  $K$ - $\epsilon$  model which appeared to suggest that the main source of the errors could be due to the use of an isotropic eddy-viscosity in the standard  $K$ - $\epsilon$  model. Later, So *et al.*<sup>9</sup> presented results which seemed to indicate that the right near wall model could significantly improve the predictions of the  $K$ - $\epsilon$  model for the backstep problem. Similar claims were made by Karniadakis *et al.*<sup>10</sup> who argued that the new near wall treatment in their RNG based  $K$ - $\epsilon$  model gave rise to drastically improved predictions for the reattachment point. However, Avva, Kline and Ferziger<sup>11</sup> presented results which suggested that the large underprediction of the reattachment point attributed to the standard  $K$ - $\epsilon$  model was due mainly to the fact that the previously reported computations were under-resolved. When sufficient resolution was used, they found that the actual

error was only of the order of 10% — a deficiency which they eliminated by introducing an empirical correlation for streamline curvature. Considering the need to accurately predict separated turbulent flows — which can have a wealth of important scientific and engineering applications — it is rather unsettling that such a wide range of conflicting claims still permeate the literature. This establishes the motivation of the present paper which is to attempt to clarify this issue.

In this paper, the following questions will be addressed:

- 1) Precisely what does the standard  $K$ - $\epsilon$  model predict for this backstep problem when the numerics are done properly to insure full resolution of the flowfield and accurate implementation of the boundary conditions,
- 2) What is the physical source of actual errors in the standard  $K$ - $\epsilon$  model, and
- 3) Can these errors be eliminated within the framework of two-equation turbulence models without the *ad hoc* adjustment of constants or the introduction of other arbitrary empiricisms?

These questions will be addressed by conducting sufficiently resolved computations of the standard and anisotropic  $K$ - $\epsilon$  model — with several different wall boundary conditions — for the backstep configuration of Kim *et al.*<sup>2</sup> and Eaton and Johnston<sup>3</sup>. By making detailed comparisons with the experiments, it will be demonstrated that the standard  $K$ - $\epsilon$  model yields results that are within 12% of the experimental data. With the introduction of an anisotropic eddy viscosity, calibrated independently without any *ad hoc* empiricisms, the  $K$ - $\epsilon$  model is shown to yield an exceptionally good prediction for the reattachment point that is within a few percent of the experimental result. The physical implications that these results have on the previous work cited above, as well as on future applications to more complex separated flows, will be discussed in detail in the sections to follow.

## 2. FORMULATION OF THE PHYSICAL PROBLEM

The problem to be considered is the fully-developed turbulent flow of an incompressible viscous fluid past a backward-facing step (a schematic is provided in figure 1). Calculations will be conducted for the Kim *et al.*<sup>2</sup> configuration wherein the expansion ratio (step height: outlet channel height)  $E$  is 1:3 and the Reynolds number  $Re = 132,000$  based on the inlet centerline mean velocity and outlet channel height. The Reynolds averaged Navier-Stokes and continuity equations are solved which take the form:

$$\frac{\partial \bar{u}}{\partial x} + \frac{\partial \bar{v}}{\partial y} = 0 \quad (1)$$

$$\frac{\partial \bar{u}}{\partial t} + \bar{u} \frac{\partial \bar{u}}{\partial x} + \bar{v} \frac{\partial \bar{u}}{\partial y} = -\frac{\partial \bar{p}}{\partial x} + \nu \left( \frac{\partial^2 \bar{u}}{\partial x^2} + \frac{\partial^2 \bar{u}}{\partial y^2} \right) - \frac{\partial \tau_{xx}}{\partial x} - \frac{\partial \tau_{xy}}{\partial y} \quad (2)$$

$$\frac{\partial \bar{v}}{\partial t} + \bar{u} \frac{\partial \bar{v}}{\partial x} + \bar{v} \frac{\partial \bar{v}}{\partial y} = -\frac{\partial \bar{p}}{\partial y} + \nu \left( \frac{\partial^2 \bar{v}}{\partial x^2} + \frac{\partial^2 \bar{v}}{\partial y^2} \right) - \frac{\partial \tau_{xy}}{\partial x} - \frac{\partial \tau_{yy}}{\partial y} \quad (3)$$

where,  $\bar{u}$  and  $\bar{v}$  are the mean velocity components in the  $x$  and  $y$  directions;  $\bar{p}$  is the modified mean pressure;  $\tau_{xx}$ ,  $\tau_{xy}$  and  $\tau_{yy}$  are the components of the Reynolds stress tensor  $\tau_{ij} \equiv \overline{u'_i u'_j}$ ; and  $\nu$  is the kinematic viscosity. In the standard  $K$ - $\epsilon$  model with isotropic eddy-viscosity the Reynolds stress tensor takes the form (see Launder and Spalding<sup>12</sup>)

$$\tau_{ij} = \frac{2}{3} K \delta_{ij} - 2 C_\mu \frac{K^2}{\epsilon} \bar{S}_{ij} \quad (4)$$

where

$$\bar{S}_{ij} = \frac{1}{2} \left( \frac{\partial \bar{u}_i}{\partial x_j} + \frac{\partial \bar{u}_j}{\partial x_i} \right) \quad (5)$$

is the mean rate of strain tensor,  $K \equiv \frac{1}{2} \tau_{ii}$  is the turbulent kinetic energy,  $\epsilon$  is the turbulent dissipation rate,  $\bar{u}_i = (\bar{u}, \bar{v})$  is the mean velocity vector, and  $C_\mu$  is a dimensionless constant which is

taken to be 0.09. An anisotropic  $K$ - $\epsilon$  model will be considered — namely, the nonlinear  $K$ - $\epsilon$  model of Speziale<sup>8</sup> — wherein the Reynolds stress tensor takes the form

$$\tau_{ij} = \frac{2}{3}K\delta_{ij} - 2C_\mu \frac{K^2}{\epsilon} \bar{S}_{ij} - 4C_D C_\mu^2 \frac{K^3}{\epsilon^2} (\overset{\circ}{\bar{S}}_{ij} - \frac{1}{3}\overset{\circ}{\bar{S}}_{kk}\delta_{ij} + \bar{S}_{ik}\bar{S}_{kj} - \frac{1}{3}\bar{S}_{kl}\bar{S}_{kl}\delta_{ij}) \quad (6)$$

where

$$\overset{\circ}{\bar{S}}_{ij} = \frac{\partial \bar{S}_{ij}}{\partial t} + \bar{u}_k \frac{\partial \bar{S}_{ij}}{\partial x_k} - \frac{\partial \bar{u}_i}{\partial x_k} \bar{S}_{kj} - \frac{\partial \bar{u}_j}{\partial x_k} \bar{S}_{ki} \quad (7)$$

is the frame-indifferent Oldroyd derivative and  $C_D$  is a dimensionless constant which takes on the value of 1.68 based on a calibration with turbulent channel flow data. The standard  $K$ - $\epsilon$  model is recovered in the limit as  $C_D \rightarrow 0$ . Both the standard and anisotropic  $K$ - $\epsilon$  model are solved in conjunction with modeled transport equations for the turbulent kinetic energy  $K$  and turbulent dissipation rate  $\epsilon$  given by<sup>12</sup>

$$\frac{\partial K}{\partial t} + \bar{u} \frac{\partial K}{\partial x} + \bar{v} \frac{\partial K}{\partial y} = \mathcal{P} - \epsilon + \frac{\partial}{\partial x} \left[ \left( v + \frac{v_T}{\sigma_K} \right) \frac{\partial K}{\partial x} \right] + \frac{\partial}{\partial y} \left[ \left( v + \frac{v_T}{\sigma_K} \right) \frac{\partial K}{\partial y} \right] \quad (8)$$

$$\frac{\partial \epsilon}{\partial t} + \bar{u} \frac{\partial \epsilon}{\partial x} + \bar{v} \frac{\partial \epsilon}{\partial y} = C_{\epsilon 1} \frac{\epsilon}{K} \mathcal{P} - C_{\epsilon 2} \frac{\epsilon^2}{K} + \frac{\partial}{\partial x} \left[ \left( v + \frac{v_T}{\sigma_\epsilon} \right) \frac{\partial \epsilon}{\partial x} \right] + \frac{\partial}{\partial y} \left[ \left( v + \frac{v_T}{\sigma_\epsilon} \right) \frac{\partial \epsilon}{\partial y} \right] \quad (9)$$

where  $v_T \equiv C_\mu \frac{K^2}{\epsilon}$  is the eddy viscosity,

$$\mathcal{P} = -\tau_{xx} \frac{\partial \bar{u}}{\partial x} - \tau_{xy} \left( \frac{\partial \bar{u}}{\partial y} + \frac{\partial \bar{v}}{\partial x} \right) - \tau_{yy} \frac{\partial \bar{v}}{\partial y}$$

is the turbulence production, and  $C_{\epsilon 1}$ ,  $C_{\epsilon 2}$ ,  $\sigma_K$  and  $\sigma_\epsilon$  are dimensionless constants which, respectively, are taken to be 1.44, 1.92, 1.0 and 1.3. The Reynolds averaged equations (1)-(7) are solved subject to the following boundary conditions:

- (a) inlet profiles for  $\bar{u}$ ,  $K$  and  $\epsilon$  are specified five step heights upstream of the step corner ( $\bar{u}$  is taken from the experimental data<sup>3</sup> and the corresponding profiles for  $K$  and  $\epsilon$  are computed from the

model formulated for channel flow),

(b) the law of the wall is used at the upper and the lower walls, and

(c) standard extrapolated outflow conditions are applied thirty step heights downstream of the step corner.

The law of the wall is applied in two different forms. In the standard two-layer form of the law of the wall:

$$\bar{u}^+ = \frac{1}{\kappa} \ln y^+ + 5, \quad \frac{K}{u_\tau^2} = C_\mu^{-1/2}, \quad \epsilon = C_\mu^{3/4} \frac{K^{3/2}}{y} \quad (10)$$

at the first grid point  $y$  away from the wall if  $y^+ \equiv y u_\tau / \nu \geq 11.6$  given that  $\bar{u}^+ = \bar{u} / u_\tau$  ( $u_\tau$  is the shear velocity and  $\kappa = 0.41$  is the von Kármán constant); if  $y^+ < 11.6$ , then  $\bar{u}$ ,  $K$  and  $\epsilon$  are interpolated to their wall values based on viscous sublayer constraints.<sup>13</sup> A three-layer law of the wall where

$$\bar{u}^+ = \begin{cases} y^+, & \text{for } y^+ \leq 5 \\ -3.05 + 5 \ln y^+, & \text{for } 5 < y^+ \leq 30 \\ 5.5 + 2.5 \ln y^+, & \text{for } y^+ > 30 \end{cases} \quad (11)$$

is also implemented along the lines of Avva *et al.*<sup>11</sup> wherein the fact that the normal derivative of  $K$  vanishes at the wall is made use of along with more elaborate interpolation formulas for  $K$  and  $\epsilon$  (see, also, Amano<sup>13</sup> for a detailed discussion). It must be said at the outset that the law of the wall does not formally apply to separated turbulent boundary layers. However, since the separation point is fixed at the corner of the backstep — and the flowfield is solved iteratively so that the shear velocity  $u_\tau$  can be updated until it converges — major errors do not appear to result from its use as will be demonstrated in the next section.

The governing equations (1)-(7) are solved using a finite volume method (see Lilley and Rhode<sup>14</sup> and Thangam and Hur<sup>15</sup>). Here we are interested in the steady state solution which is ob-

tained by solving the system of algebraic equations by a line relaxation method<sup>14</sup> with the repeated application of the tridiagonal matrix solution algorithm.<sup>16</sup> The issue of resolution is crucial for the backstep problem. As discussed by Avva *et al.*,<sup>11</sup> several researchers have reported results that were in severe error due to a lack of adequate resolution. Thangam and Hur<sup>15</sup> conducted a careful grid refinement study based on this finite volume method for grids containing 150×75 to 400×200 mesh points (these meshes have variable grid spacing to allow for maximum resolution near the step corner and the walls). The conclusion of their study was that a 200×100 mesh yielded results that were within 0.3% of the grid independent solution; the use of significantly coarser meshes could lead to appreciable errors whereas, for the most part, the improvement to be gained by the use of finer meshes would be minimal. All of the computations conducted in this study were performed using this 200×100 nonuniform mesh. As indicated earlier, the inlet conditions were specified 5 step heights upstream of the step corner and the outlet boundary conditions were specified 30 step heights downstream of the step corner. It is crucial that a sufficient distance downstream of the reattachment point be allowed before the outflow conditions are imposed. Many earlier computations of the backstep problem were in significant error due to the imposition of fully-developed outflow conditions too close to the reattachment point.

The steady state solution of Eqs. (1)-(7) is obtained by an iterative solution of the discretized equations. The computed solution was assumed to have converged to its steady state when the root mean square of the average difference between successive iterations was less than  $10^{-4}$  for the mass source.<sup>14,15</sup> Approximately 2000 iterations were needed for the convergence of the standard  $K-\epsilon$  model; this corresponds to approximately 30 minutes of CPU time in a partially vectorized mode on the CRAY-2S supercomputer using 64-bit precision. The anisotropic  $K-\epsilon$  model requires approximately 30% more CPU time due to the fact that the additional correction terms to the standard  $K-\epsilon$  model have to be evaluated during each iteration. These correction terms are dispersive rather than being dissipative — an additional feature that slows convergence.

### 3. DISCUSSION OF THE RESULTS

First, results will be presented for the standard  $K$ - $\epsilon$  model using the two-layer law of the wall boundary conditions. For this case — as well as the other results to follow — computed results for the mean velocity streamlines, the streamwise mean velocity profiles, the streamwise turbulence intensity profiles and the turbulence shear stress profiles will be compared with the Kim *et al.*<sup>2</sup> experimental data as updated by Eaton and Johnston.<sup>3</sup> In figure 2(a) the computed streamlines are shown which indicate reattachment at  $X/H \approx 6.0$  — a result which is approximately a 15% underprediction of the experimental reattachment point of  $X/H \approx 7.1$ . This is in contrast to earlier reported results which seemed to indicate that the standard  $K$ - $\epsilon$  model underpredicts the reattachment point by 20-25% — an exaggerated underprediction due to the lack of adequate resolution in those computations. (A spurious underprediction of the reattachment point can also result from the application of outflow boundary conditions at a distance  $X/H < 25$  from the step corner as some authors have done). In figure 2(b), the streamwise mean velocity profiles predicted by the standard  $K$ - $\epsilon$  model are compared with the experimental data. Except in the vicinity of the reattachment point, the comparisons are fairly good. More serious discrepancies between the model predictions and the experimental data occur in the initial part of the recovery zone for the streamwise turbulence intensity profiles as shown in figure 3(a). However, the model predictions for the turbulence shear stress profiles are reasonably good as can be seen from figure 3(b).

Next, we will examine the effect of the near wall modeling. In figures 4(a)-(b), the mean flow streamlines and streamwise mean velocity profiles obtained from the standard  $K$ - $\epsilon$  model with the three layer law of the wall boundary condition is shown. With this more accurate version of the law of the wall, the standard  $K$ - $\epsilon$  model predicts reattachment at  $X/H \approx 6.25$  — a result which is extremely close to that reported by Avva *et al.*<sup>11</sup> By integrating the  $K$ - $\epsilon$  model directly to the wall — with an asymptotically consistent low Reynolds number correction (cf., So *et al.*<sup>9</sup> and Speziale *et al.*<sup>17</sup>) — it is possible to improve the prediction for the reattachment point by approximately 5%. Some earlier published work claiming that the near wall modeling could make a larger difference

were in all likelihood due to inadequate resolution of the computations (e.g., So *et al.*<sup>9</sup> used a 93×66 mesh). Considering the current state of development of near wall modeling — as well as the relatively small benefits that it can yield for the backstep problem — the remaining results to be shown will be based on the three-layer law of the wall boundary condition. However, for turbulent flows where the separation point is *not fixed*, near wall turbulence modeling can play a much more important role.

Now, it will be demonstrated that the use of the anisotropic eddy-viscosity model (6) can yield a more significant improvement in the results. The computed mean velocity streamlines obtained from the nonlinear  $K$ - $\epsilon$  model are shown in figure 6(a). They indicate reattachment at  $X/H \approx 6.9$ : a result that is within 3% of the mean experimental value of  $X/H \approx 7.1$ . This more accurate prediction of the reattachment point is reflected in the streamwise mean velocity profiles shown in figure 6(b) which are in better agreement with the experimental data<sup>2,3</sup> than those obtained from the standard  $K$ - $\epsilon$  model based on an isotropic eddy viscosity. Some of the earlier reported results for the nonlinear  $K$ - $\epsilon$  model (see Speziale<sup>8</sup> and Speziale and Ngo<sup>18</sup>) were lower due to insufficient numerical resolution of the flowfield. The corresponding streamwise turbulence intensity profiles and turbulence shear stress profiles are compared with the experimental data in figure 7(a)-(b). On balance, the agreement between the model predictions and experimental data is good (it must be remembered that the uncertainty in the turbulence Reynolds stress measurements is of the order of 10%). The most notable difference between the predictions of the anisotropic and the standard  $K$ - $\epsilon$  model lies in the streamwise turbulence intensity located approximately one step height above the corner of the step. Unlike the standard  $K$ - $\epsilon$  model, the nonlinear  $K$ - $\epsilon$  model predicts a dramatic trough in this region — a result that is consistent with the more recent independent experiments.<sup>19,20</sup> In fact, it is the more accurate prediction of the normal Reynolds stress difference  $\tau_{yy} - \tau_{xx}$  that accounts for the better predictions of the nonlinear  $K$ - $\epsilon$  model. This can be illustrated directly in turbulent channel flow. In figure 8, the normal Reynolds stress difference predicted by the nonlinear  $K$ - $\epsilon$  model is compared with the experimental data of Laufer.<sup>21</sup> It is clear that the

nonlinear  $K$ - $\epsilon$  model does a reasonably good job of reproducing the experimental data whereas the standard  $K$ - $\epsilon$  model erroneously predicts that  $\tau_{yy} - \tau_{xx} = 0$ . The accurate prediction of this normal Reynolds stress difference is important in the backstep problem since the mean flow streamfunction  $\bar{\psi}$  (where  $\bar{u} \equiv -\partial\bar{\psi}/\partial y$ , and  $\bar{v} \equiv \partial\bar{\psi}/\partial x$ ) is a solution of the transport equation<sup>18</sup>

$$\bar{u} \frac{\partial}{\partial x} (\nabla^2 \bar{\psi}) + \bar{v} \frac{\partial}{\partial y} (\nabla^2 \bar{\psi}) = \nu \nabla^4 \bar{\psi} - \frac{\partial^2 (\tau_{yy} - \tau_{xx})}{\partial x \partial y} - \frac{\partial^2 \tau_{xy}}{\partial x^2} + \frac{\partial^2 \tau_{xy}}{\partial y^2} \quad (12)$$

and, hence, the normal Reynolds stress difference  $\tau_{yy} - \tau_{xx}$  contributes directly to the calculation of the mean velocity field. This is the case for any flow with streamline curvature since the normal Reynolds stress term on the r.h.s. of (12) can be converted to the alternate form

$$\frac{\partial^2 (\tau_{nn} - \tau_{ss})}{\partial n \partial s}$$

in terms of an intrinsic coordinate system where  $n$  and  $s$  are, respectively, the normal and tangential directions along a streamline.

Finally, we will examine the RNG based  $K$ - $\epsilon$  model of Yakhot and Orszag.<sup>22</sup> For high turbulence Reynolds numbers, it is of the same general form as the standard  $K$ - $\epsilon$  model given by Eqs. (4), (8) and (9). However, the numerical values of the constants — which are computed by the RNG approach — take on the alternate values:

$$C_\mu = 0.0837, \quad C_{\epsilon 1} = 1.063, \quad C_{\epsilon 2} = 1.7215$$

$$\sigma_K = 0.7179, \quad \sigma_\epsilon = 0.7179, \quad \kappa = 0.372$$

For the low turbulence Reynolds numbers which occur close to the walls in this backstep problem, the RNG  $K$ - $\epsilon$  model has a built-in correction that allows for a direct integration to a solid boundary with the no-slip condition applied. However, we found this near wall correction to be rather ambiguous — especially in the presence of geometrical discontinuities such as those which occur near the backstep corners. Hence, we will present results in which we match to the three-layer law of

the wall. In figures 9(a)-(b), the mean flow streamlines and the streamwise mean velocity profiles obtained from the RNG  $K-\epsilon$  model are shown. The RNG  $K-\epsilon$  model predicts reattachment at  $X/H \approx 4$  — a result that constitutes a substantial underprediction of the experimental reattachment point of  $X/H \approx 7.1$ . Due to this significant underprediction of the reattachment point, the streamwise turbulence intensity and turbulence shear stress profiles predicted by the RNG  $K-\epsilon$  model are in serious error as illustrated in figures 10(a)-(b). The origin of this substantial underprediction of the reattachment point lies in the choice of  $C_{\epsilon 1} = 1.063$ . In a homogeneous shear flow, it can be shown that the eddy viscosity

$$\nu_T \sim \exp(\lambda t^*) \quad (13)$$

where  $t^*$  is the time (nondimensionalized by the shear rate) and  $\lambda$  is the growth rate given by<sup>23</sup>

$$\lambda = \left[ \frac{C_\mu (C_{\epsilon 2} - C_{\epsilon 1})^2}{(C_{\epsilon 1} - 1)(C_{\epsilon 2} - 1)} \right]^{1/2} \quad (14)$$

Hence the growth rate of the eddy viscosity becomes singular as  $C_{\epsilon 1} \rightarrow 1$ . For  $C_{\epsilon 1} = 1.063$  — as opposed to the more standard value of  $C_{\epsilon 1} = 1.44$  — the growth rate of the eddy viscosity will be overly large. An overprediction of the eddy viscosity will make the model too dissipative — a feature which will cause the separation bubble to shorten as shown in figure 9(a). Hence, while the use of an alternate near wall treatment with the RNG  $K-\epsilon$  model could cause the separation bubble to become slightly larger, we feel that it is very unlikely that a reattachment point close to  $X/H \approx 7$  could be obtained from this RNG  $K-\epsilon$  model as reported in Karniadakis *et al.*<sup>10</sup> (We believe that the calculations of Karniadakis *et al.*<sup>10</sup> may have been under-resolved). It should be noted, however, that Smith and Yakhot<sup>24</sup> have recently determined that there may have been an error in the original calculation of  $C_{\epsilon 1}$  by Yakhot and Orszag<sup>22</sup>; they obtained an alternate value of  $C_{\epsilon 1} = 1.40$ . With this higher value of  $C_{\epsilon 1}$  — and with the use of an RNG based anisotropic eddy-viscosity (see Rubinstein and Barton<sup>25</sup>) — there is no question that the RNG  $K-\epsilon$  model would yield excellent results for the backstep problem.

#### 4. CONCLUSIONS

A reasonably detailed theoretical and computational analysis of the performance of two-equation turbulence models for turbulent flow past a backward facing step has been presented in an effort to resolve numerous conflicting studies that have been published during the past ten years. The following general conclusions were arrived at:

- 1) The standard  $K$ - $\epsilon$  model with three-layer wall functions predicts reattachment at  $X/H \approx 6.25$  — a result that is within 12% of the experimental value of Kim, Kline and Johnston<sup>2</sup> for this backstep problem. This result is in close agreement with the recent computations of Avva *et al.*<sup>11</sup> and hence there is little doubt that earlier studies which attributed a 20-25% underprediction of the reattachment point to the standard  $K$ - $\epsilon$  model were in error due to inadequate numerical resolution of the flowfield.
- 2) When the standard  $K$ - $\epsilon$  model is appropriately modified to include an anisotropic eddy viscosity,<sup>8</sup> the reattachment point moves out to  $X/H \approx 6.9$ . This result, as well as the other mean velocity statistics, are within 3% of the experimental data — an improvement due to the more accurate prediction of normal Reynolds stress differences.
- 3) The RNG  $K$ - $\epsilon$  model of Yakhot and Orszag<sup>22</sup> substantially underpredicts the reattachment point. This problem arises since  $C_{\epsilon 1}$  is too close to 1 — a feature that causes the model to be overly dissipative (e.g., when  $C_{\epsilon 1} = 1$ , the growth rate of the eddy viscosity becomes singular in homogeneous shear flow). The previously published results of Karniadakis *et al.*,<sup>10</sup> to the contrary, appear to have been under-resolved. However, there is no question that with the recent suggested correction (Smith and Yakhot<sup>24</sup>) of  $C_{\epsilon 1}$  to 1.40 — and with the use of an anisotropic eddy viscosity — the RNG  $K$ - $\epsilon$  model would yield excellent results for the backstep problem.

Finally, some remarks are in order concerning the implications that these results have on turbulence modeling. The deficiencies of two-equation models are well established, particularly in turbulent flows with body forces or Reynolds stress relaxation effects.<sup>23</sup> Consequently, the find-

ings of this study should not be interpreted as an unequivocal endorsement of two-equation models. Nonetheless, this study certainly does indicate that properly calibrated two-equation turbulence models, with an anisotropic eddy viscosity, can yield excellent results for the backstep problem that are far superior to the results obtained from the older zero or one equation models.

## References

1. S.J. Kline, B.J. Cantwell, and G.M. Lilley, eds., *Proceedings of the 1980-81 AFOSR-HTTM Stanford Conference on Complex Turbulent Flows*, Stanford University Press, Stanford, CA (1981).
2. J. Kim, S.J. Kline, and J.P. Johnston, *ASME Journal of Fluids Engineering*, **102**, 302 (1980).
3. J. Eaton and J.P. Johnston, *Technical Report MD-39*, Stanford University, CA (1980).
4. M.M.S. Sindir, *Ph. D. Thesis*, University of California – Davis (1982).
5. M.M. Gibson, *Int. J. Heat and Mass Transfer*, **21**, 1609 (1981).
6. C.P. Chen, *NASA Report CR-178536* (1985).
7. K. Hanjalic, B.E. Launder, and R. Schiestel, in *Turbulent Shear Flows 2* (L.J.S. Bradbury *et al.*, eds.) Springer-Verlag, New York (1980).
8. C.G. Speziale, *J. Fluid Mech.*, **178**, 459 (1987).
9. R.M.C. So, Y.G. Lai, B.C. Hwang, and G.J. Yao, *ZAMP*, **39**, 13 (1988).
10. G. Karniadakis, A. Yakhot, S. Rakib, S.A. Orszag, and V. Yakhot, *Proceedings of the Seventh Symposium on Turbulent Shear Flows*, Stanford University Press, CA (1989).
11. R.K. Avva, S.J. Kline and J.H. Ferziger, *Technical Report TF-33*, Stanford University, CA (1988).
12. B.E. Launder and D.B. Spalding, *Computer Meth. Appl. Mech. & Eng.*, **3**, 269 (1974).
13. R.S. Amano, *Num. Heat Transfer*, **7**, 59 (1984).
14. D.G. Lilley and D.L. Rhode, *NASA Contractor Report CR-3442* (1982).
15. S. Thangam and N. Hur, *Int. J. Eng. Sci.* (in press).
16. E. Isaacson and H.B. Keller, *Analysis of Numerical Methods*, John-Wiley, New York (1970).
17. C.G. Speziale, R. Abid, and E.C. Anderson, *AIAA Paper 81-1481* (1981).
18. C.G. Speziale and T. Ngo, *Int. J. Eng. Sci.*, **26**, 1099 (1988).
19. J.F. Meyers, S.O. Kjelgaard, and T.E. Hepner, *Fifth International Symposium on Applications of Laser Technologies to Fluid Mechanics*, Lisbon, Portugal (1990).
20. S. Thangam, S.O. Kjelgaard, C.G. Speziale, *Bull. Am. Phy. Soc.*, **35**, 2324 (1990).
21. J. Laufer, *NACA Report TN 1053* (1951).
22. V. Yakhot and S.A. Orszag, *J. Sci. Comp.*, **1**, 3 (1986).
23. C.G. Speziale, *Ann. Rev. Fluid Mech.*, **23**, 107 (1991).
24. L. Smith and V. Yakhot, *Private Communication* (1991).
25. R. Rubinstein and J.M. Barton, *Phys. Fluids A*, **2**, 1472 (1990).

## List Of Figures

Figure 1 Physical Configuration and Coordinate System.

Figure 2 Computed Flowfield for the Standard  $K-\epsilon$  Model [ $E = 1:3$ ;  $Re = 132,000$ ;  $200 \times 100$  mesh;  $C_\mu = 0.09$ ;  $C_{\epsilon 1} = 1.44$ ;  $C_{\epsilon 2} = 1.92$ ;  $\sigma_K = 1.0$ ;  $\sigma_\epsilon = 1.3$ ;  $\kappa = 0.41$ ]

a) Contours of mean streamlines

b) Mean velocity profiles at selected locations (—— computed solutions based on two layer wall model; o experiments of Kim *et al*, 1980; Eaton & Johnston, 1981)

Figure 3 Computed Turbulence Stresses for the Standard  $K-\epsilon$  Model [ $E = 1:3$ ;  $Re = 132,000$ ;  $200 \times 100$  mesh;  $C_\mu = 0.09$ ;  $C_{\epsilon 1} = 1.44$ ;  $C_{\epsilon 2} = 1.92$ ;  $\sigma_K = 1.0$ ;  $\sigma_\epsilon = 1.3$ ;  $\kappa = 0.41$ ; —— computed solutions based on two layer wall model; o experiments of Kim *et al*, 1980; Eaton & Johnston, 1981]

a) Turbulence intensity profiles

b) Turbulence shear stress profiles

Figure 4 Computed Flowfield for the Standard  $K-\epsilon$  Model [ $E = 1:3$ ;  $Re = 132,000$ ;  $200 \times 100$  mesh;  $C_\mu = 0.09$ ;  $C_{\epsilon 1} = 1.44$ ;  $C_{\epsilon 2} = 1.92$ ;  $\sigma_K = 1.0$ ;  $\sigma_\epsilon = 1.3$ ;  $\kappa = 0.41$ ]

a) Contours of mean streamlines

b) Mean velocity profiles at selected locations (—— computed solutions based on three layer wall model; o experiments of Kim *et al*, 1980; Eaton & Johnston, 1981)

Figure 5 Computed Turbulence Stresses for the Standard  $K-\epsilon$  Model [ $E = 1:3$ ;  $Re = 132,000$ ;  $200 \times 100$  mesh;  $C_\mu = 0.09$ ;  $C_{\epsilon 1} = 1.44$ ;  $C_{\epsilon 2} = 1.92$ ;  $\sigma_K = 1.0$ ;  $\sigma_\epsilon = 1.3$ ;  $\kappa = 0.41$ ; —— computed solutions based on three layer wall model; o experiments of Kim *et al*, 1980; Eaton & Johnston, 1981]

a) Turbulence intensity profiles

b) Turbulence shear stress profiles

Figure 6 Computed Flowfield for the Nonlinear  $K-\epsilon$  Model [ $E = 1:3$ ;  $Re = 132,000$ ;  $200 \times 100$  mesh;  $C_\mu = 0.09$ ;  $C_{\epsilon 1} = 1.44$ ;  $C_{\epsilon 2} = 1.92$ ;  $\sigma_K = 1.0$ ;  $\sigma_\epsilon = 1.3$ ;  $\kappa = 0.41$ ;  $C_D = C_E = 1.68$ ]

a) Contours of mean streamlines

b) Mean velocity profiles at selected locations (—— computed solutions based on three layer wall model; o experiments of Kim *et al*, 1980; Eaton & Johnston, 1981)

**Figure 7** Computed Turbulence Stresses for the Nonlinear  $K$ - $\epsilon$  Model [ $E = 1:3$ ;  $Re = 132,000$ ; 200x100 mesh;  $C_\mu = 0.09$ ;  $C_{\epsilon 1} = 1.44$ ;  $C_{\epsilon 2} = 1.92$ ;  $\sigma_K = 1.0$ ;  $\sigma_\epsilon = 1.3$ ;  $\kappa = 0.41$ ;  $C_D = C_E = 1.68$ ; ——— computed solutions based on three layer wall model; o experiments of Kim *et al*, 1980; Eaton & Johnston, 1981]

a) Turbulence intensity profiles

b) Turbulence shear stress profiles

**Figure 8** Comparison of the Computed Values of the Normal Reynolds Stress Difference Obtained from the Nonlinear  $K$ - $\epsilon$  Model with the Experimental Data of Laufer (1951) for Fully-Developed Turbulent Channel Flow. (It should be noted that the standard  $K$ - $\epsilon$  model predicts a zero normal stress difference)

**Figure 9** Computed Flowfield for the RNG  $K$ - $\epsilon$  Model [ $E = 1:3$ ;  $Re = 132,000$ ; 200x100 mesh;  $C_\mu = 0.0837$ ;  $C_{\epsilon 1} = 1.063$ ;  $C_{\epsilon 2} = 1.7215$ ;  $\sigma_K = \sigma_\epsilon = 0.7179$ ;  $\kappa = 0.372$ ]

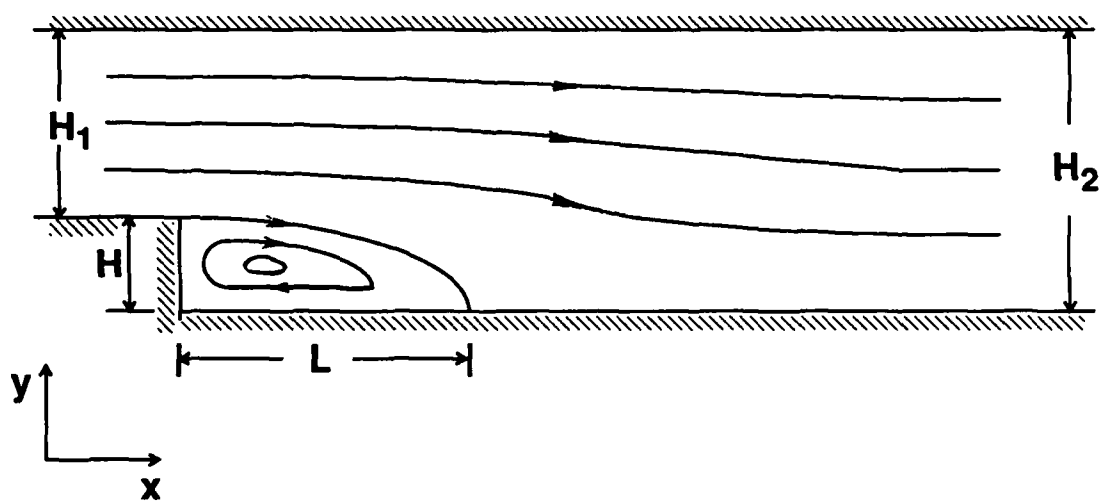
a) Contours of mean streamlines

b) Mean velocity profiles at selected locations (—— computed solutions based on three layer wall model; o experiments of Kim *et al*, 1980; Eaton & Johnston, 1981)

**Figure 10** Computed Turbulence Stresses for the RNG  $K$ - $\epsilon$  Model [ $E = 1:3$ ;  $Re = 132,000$ ; 200x100 mesh;  $C_\mu = 0.0837$ ;  $C_{\epsilon 1} = 1.063$ ;  $C_{\epsilon 2} = 1.7215$ ;  $\sigma_K = \sigma_\epsilon = 0.7179$ ;  $\kappa = 0.372$ ; ——— computed solutions based on three layer wall model; o experiments of Kim *et al*, 1980; Eaton & Johnston, 1981]

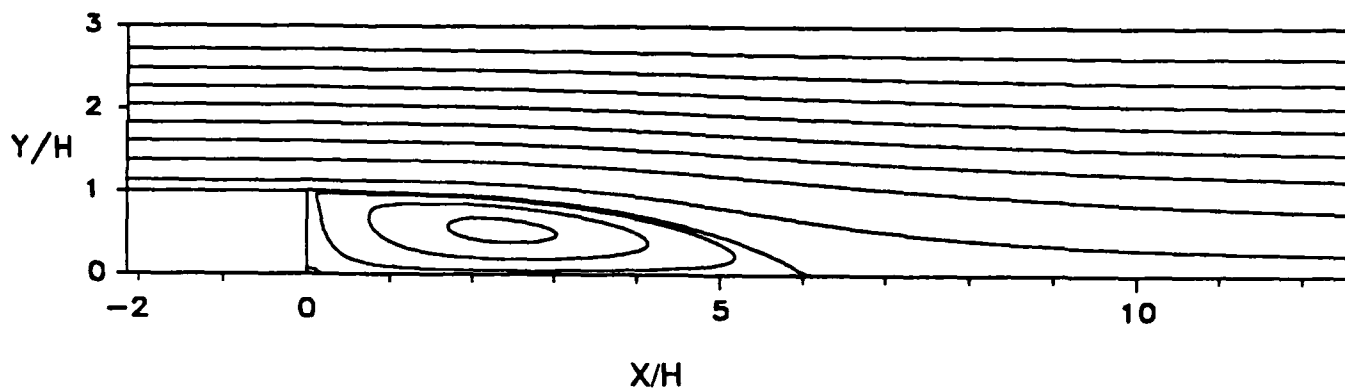
a) Turbulence intensity profiles

b) Turbulence shear stress profiles

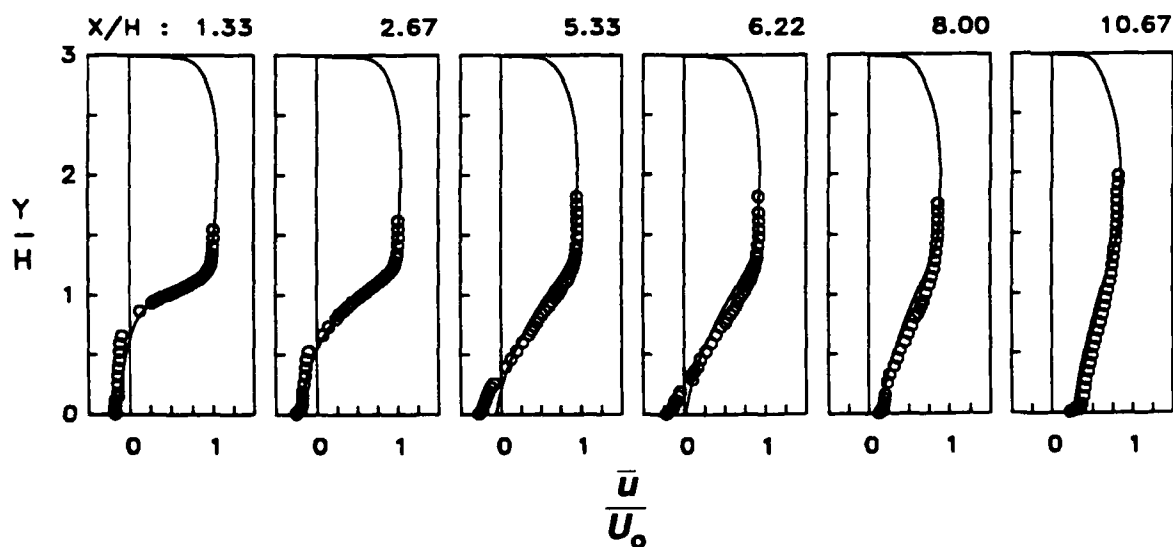


**Physical Configuration and Coordinate System**

**Figure 1**



(a) Streamlines



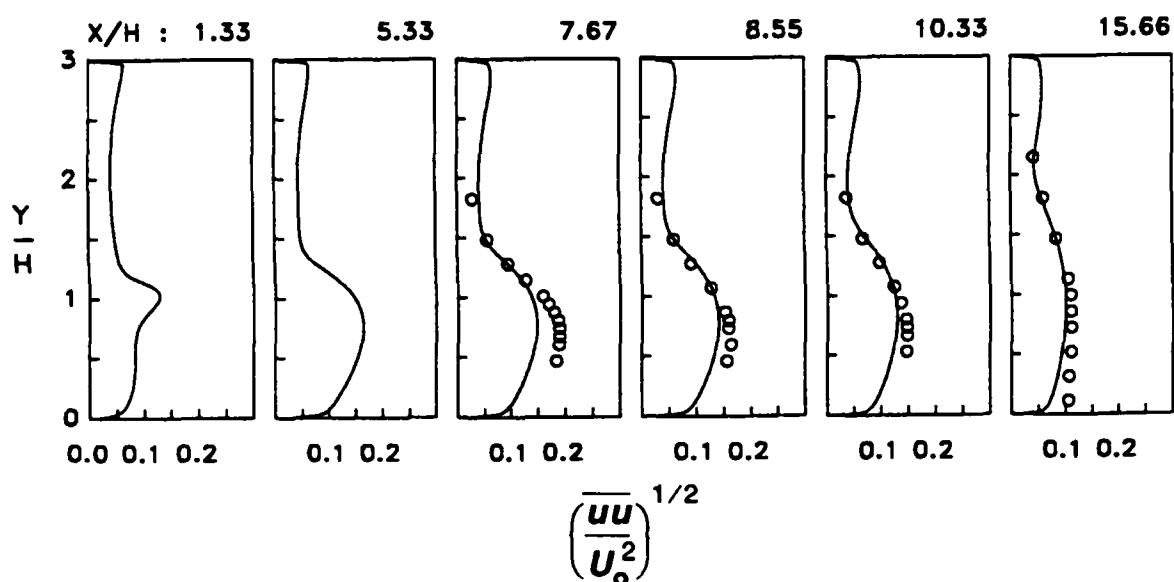
(b) Dimensionless Mean Velocity Profile

(— Computations with the two layer model  
 o Experiments of Kim *et al*, 1980; Eaton & Johnston, 1981)

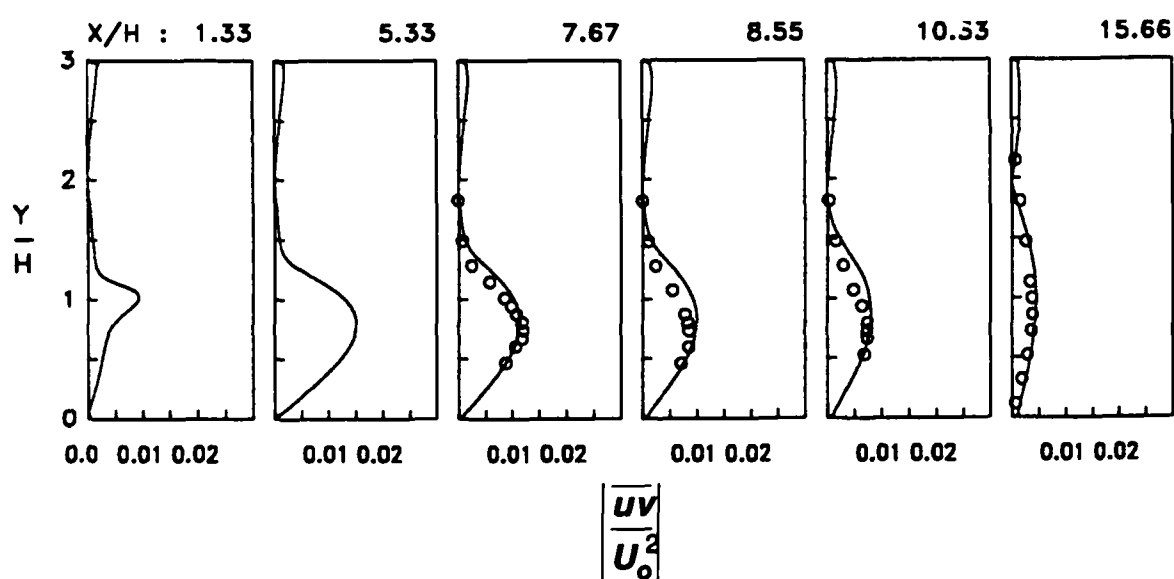
**Computed Flowfield for the Standard  $K-\epsilon$  Model**

[ $E = 1:3$ ;  $Re = 132,000$ ;  $200 \times 100$  mesh;  $C_\mu = 0.09$ ;  $C_{\epsilon 1} = 1.44$ ;  $C_{\epsilon 2} = 1.92$ ;  
 $\sigma_K = 1.0$ ;  $\sigma_\epsilon = 1.3$ ;  $\kappa = 0.41$ ]

**Figure 2**



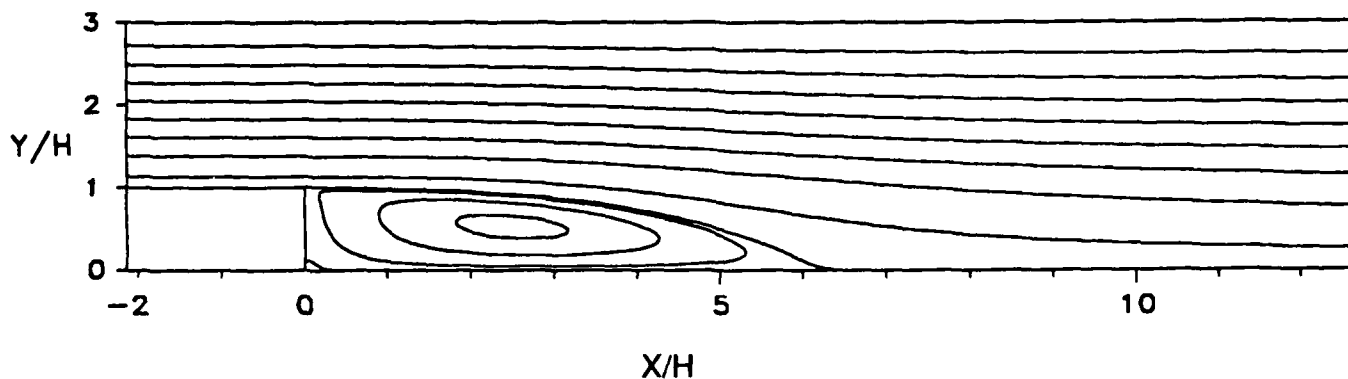
(a) Turbulence Intensity



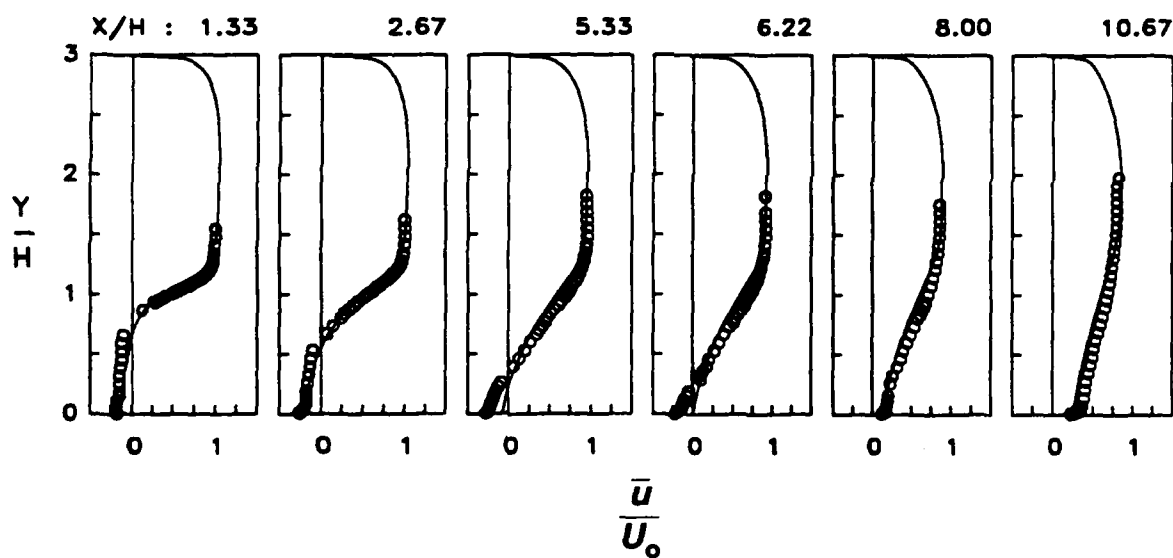
(b) Turbulence Shear Stress

**Computed Turbulence Stresses for the Standard  $K-\epsilon$  Model**  
**[ $E = 1:3$ ;  $Re = 132,000$ ;  $200 \times 100$  mesh;  $C_\mu = 0.09$ ;  $C_{\epsilon 1} = 1.44$ ;  $C_{\epsilon 2} = 1.92$ ;  
 $\sigma_K = 1.0$ ;  $\sigma_\epsilon = 1.3$ ;  $\kappa = 0.41$ ; — Computations with the two layer model;  
 $\circ$  Experiments of Kim *et al*, 1980; Eaton & Johnston, 1981]**

Figure 3



(a) Streamlines

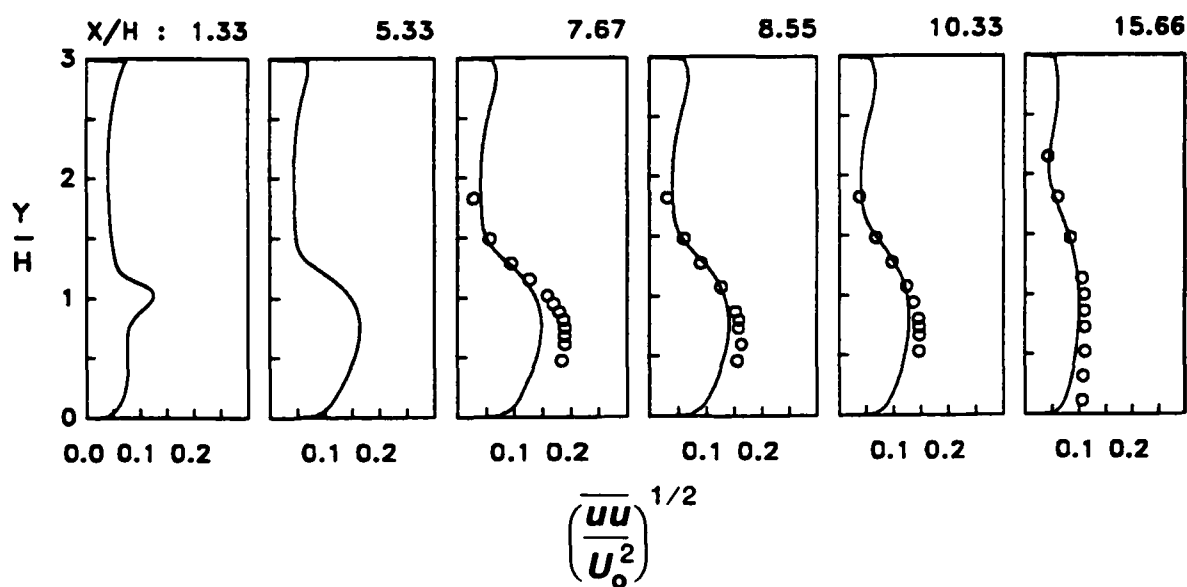


(b) Dimensionless Mean Velocity Profile

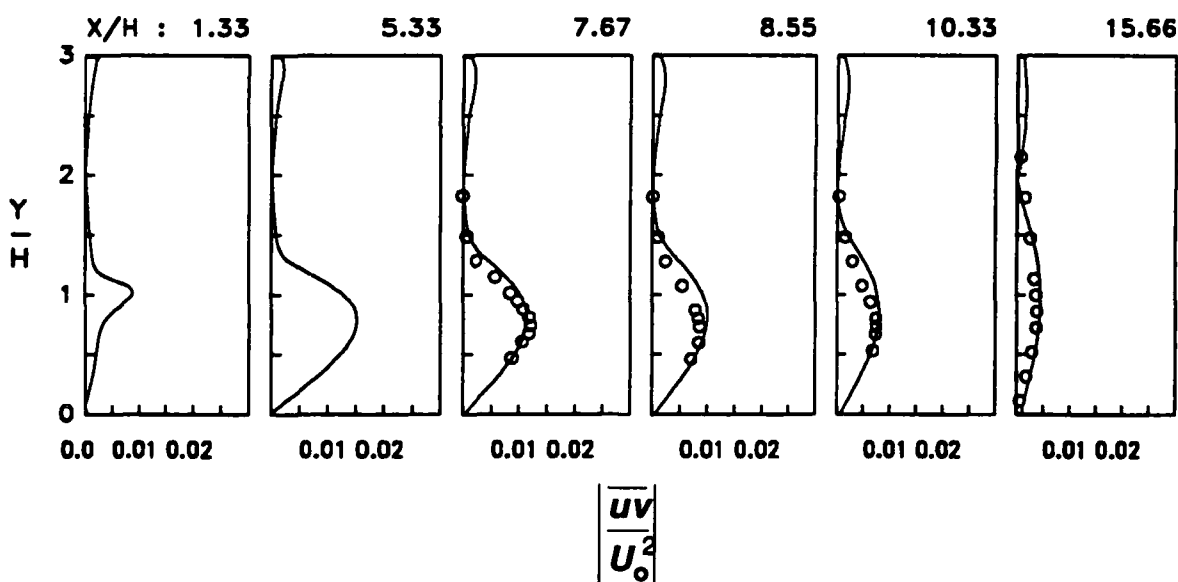
(—) Computations with the three layer model;  
 o Experiments of Kim *et al*, 1980; Eaton & Johnston, 1981)

**Computed Flowfield for the Standard  $K-\epsilon$  Model**  
 [E = 1:3; Re = 132,000; 200x100 mesh;  $C_\mu = 0.09$ ;  $C_{\epsilon 1} = 1.44$ ;  $C_{\epsilon 2} = 1.92$ ;  
 $\sigma_K = 1.0$ ;  $\sigma_\epsilon = 1.3$ ;  $\kappa = 0.41$ ]

Figure 4



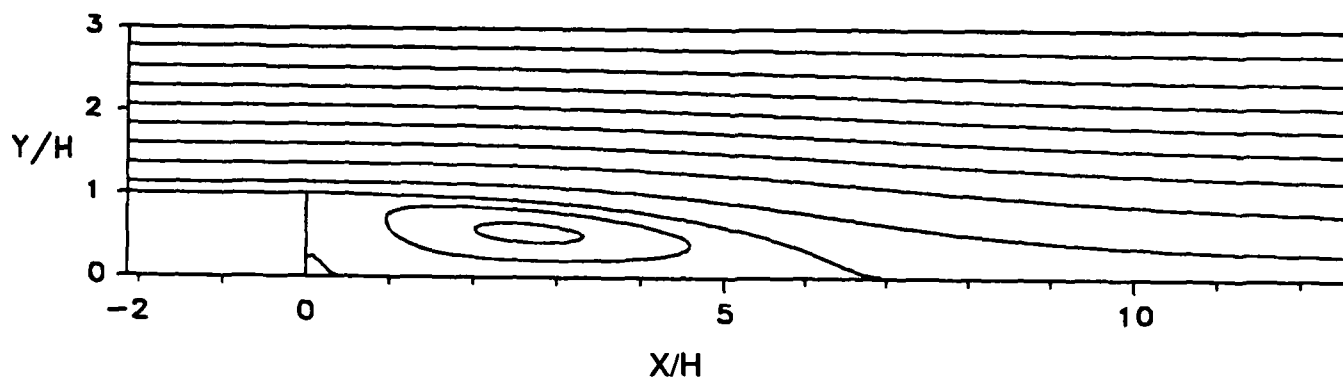
(a) Turbulence Intensity



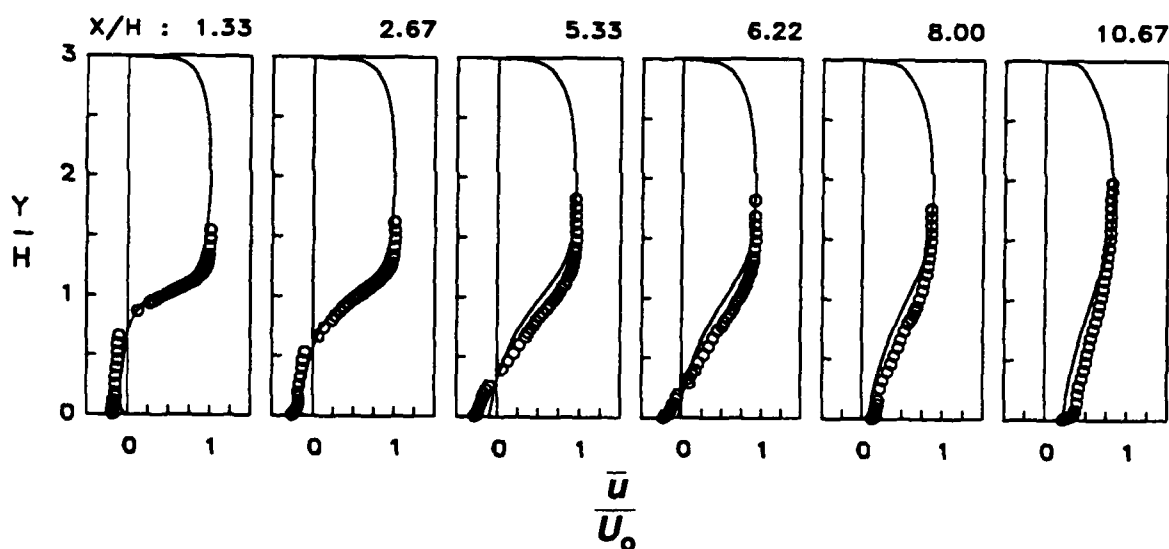
(b) Turbulence Shear Stress

**Computed Turbulence Stresses for the Standard  $K-\epsilon$  Model** [ $E = 1:3$ ;  $Re = 132,000$ ;  $200 \times 100$  mesh;  $C_\mu = 0.09$ ;  $C_{\epsilon 1} = 1.44$ ;  $C_{\epsilon 2} = 1.92$ ;  $\sigma_K = 1.0$ ;  $\sigma_\epsilon = 1.3$ ;  $\kappa = 0.41$ ; — Computations with the three layer model; o Experiments of Kim *et al*, 1980; Eaton & Johnston, 1981]

**Figure 5**



(a) Streamlines



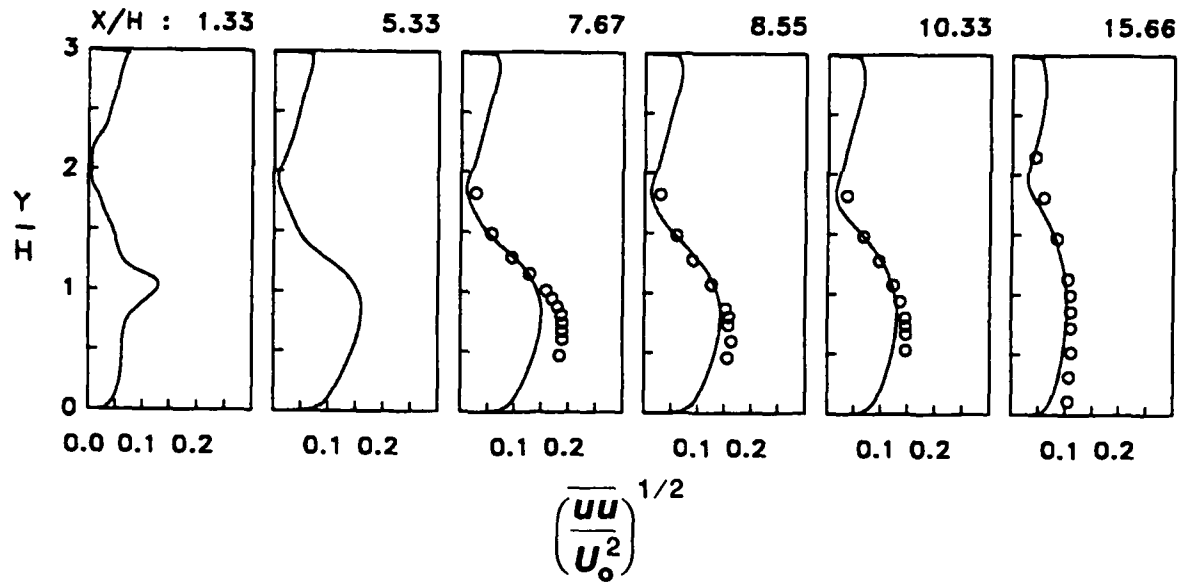
(b) Dimensionless Mean Velocity Profile

(—) Computations with the three layer model;  
 o Experiments of Kim *et al*, 1980; Eaton & Johnston, 1981)

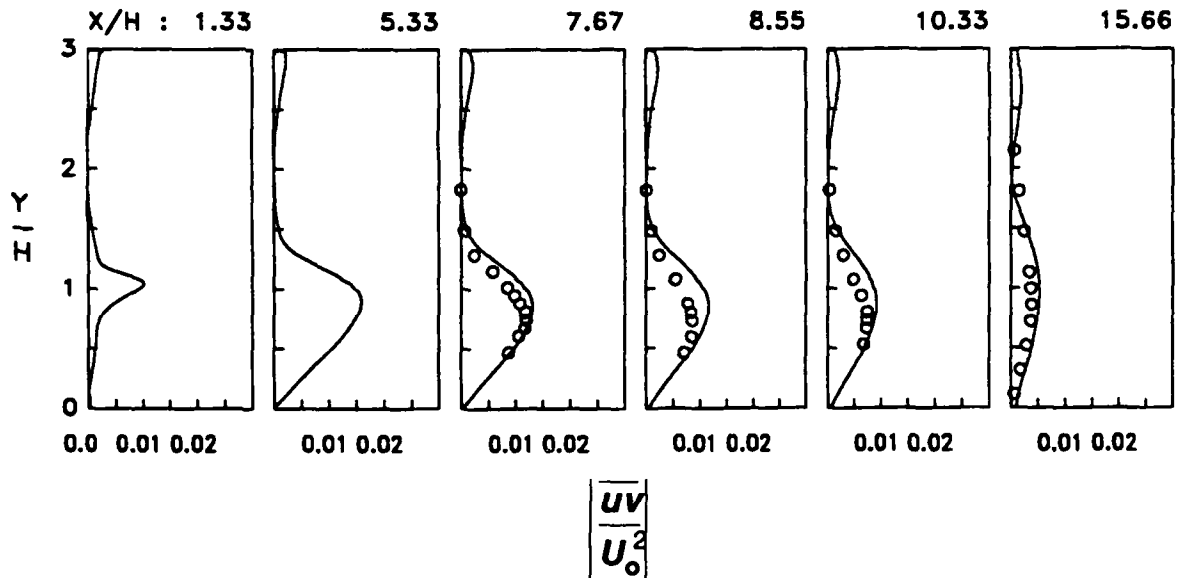
#### Computed Flowfield for the Nonlinear $K-\epsilon$ Model

[ $E = 1:3$ ;  $Re = 132,000$ ;  $200 \times 100$  mesh;  $C_\mu = 0.09$ ;  $C_{\epsilon 1} = 1.44$ ;  $C_{\epsilon 2} = 1.92$ ;  
 $\sigma_K = 1.0$ ;  $\sigma_\epsilon = 1.3$ ;  $\kappa = 0.41$ ;  $C_D = C_E = 1.68$ ]

Figure 6



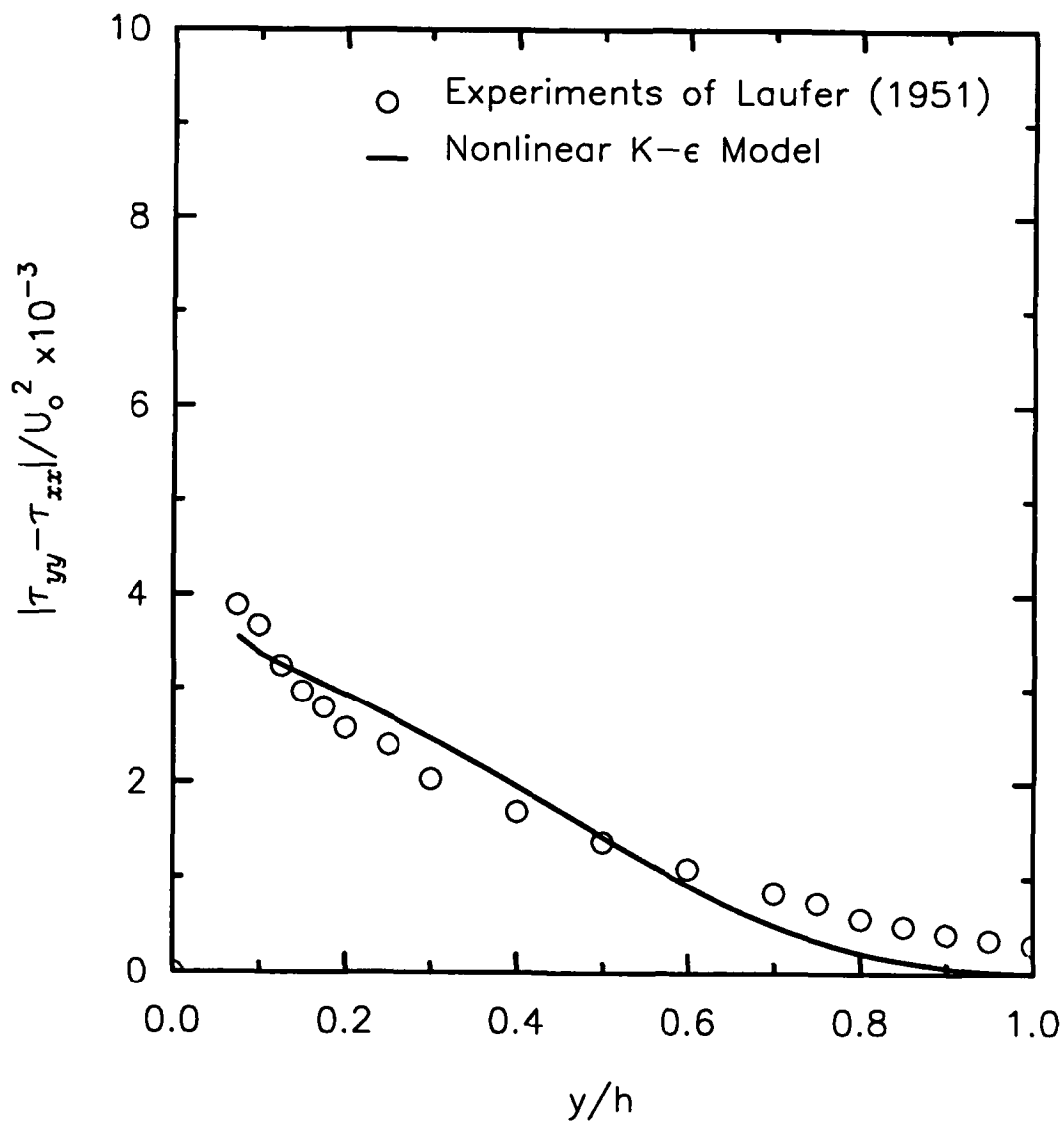
(a) Turbulence Intensity



(b) Turbulence Shear Stress

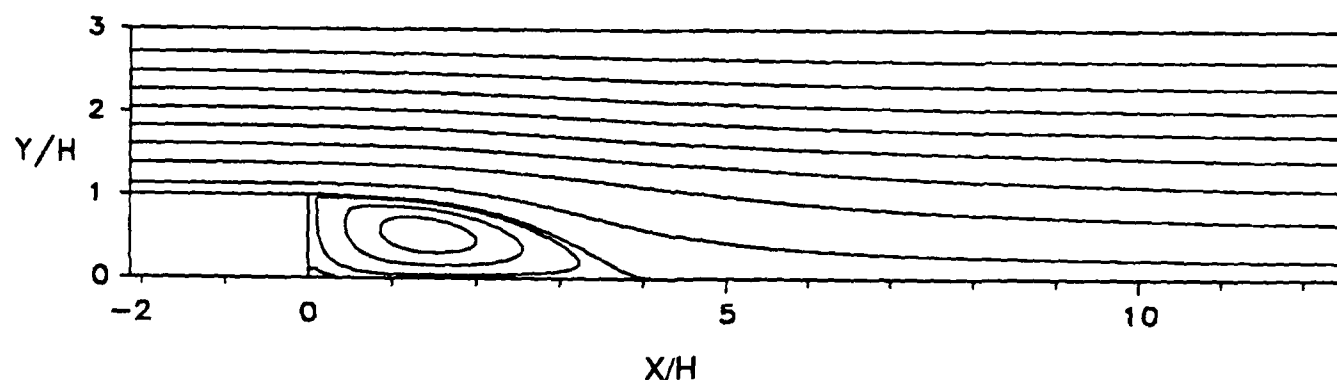
**Computed Turbulence Stresses for the Nonlinear  $K-\epsilon$  Model [ $E = 1:3$ ;  $Re = 132,000$ ;  $200 \times 100$  mesh;  $C_\mu = 0.09$ ;  $C_{\epsilon 1} = 1.44$ ;  $C_{\epsilon 2} = 1.92$ ;  $\sigma_K = 1.0$ ;  $\sigma_\epsilon = 1.3$ ;  $\kappa = 0.41$ ;  $C_D = C_E = 1.68$ ; — Computations with the three layer model; o Experiments of Kim *et al*, 1980; Eaton & Johnston, 1981]**

**Figure 7**

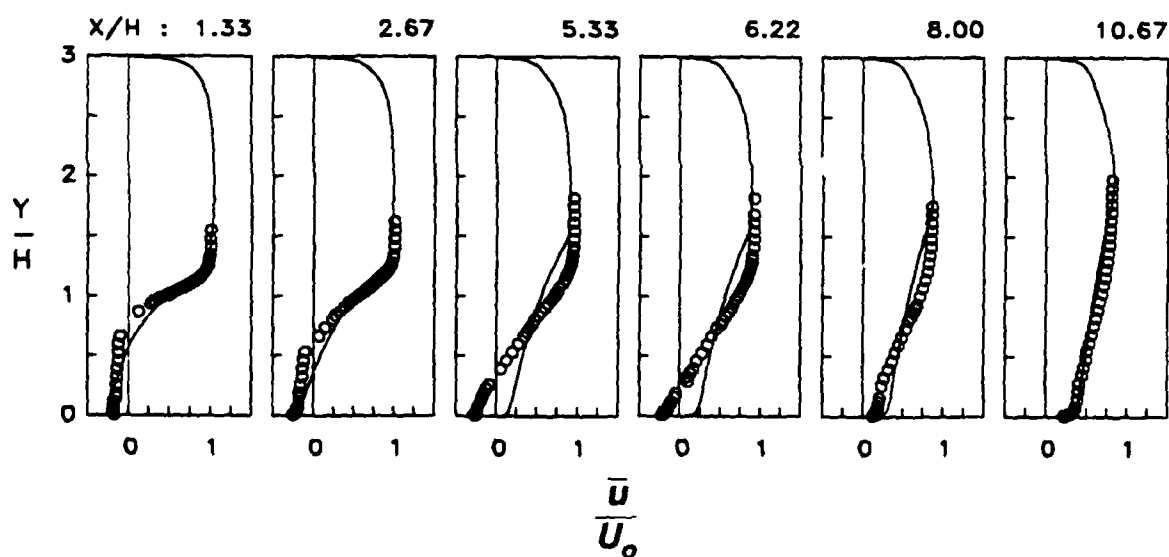


**Comparison of the computed values of the normal Reynolds stress difference obtained from the nonlinear  $K-\epsilon$  model with the experimental data of Laufer (1951) for the fully-developed turbulent channel flow. (It should be noted that the standard  $K-\epsilon$  model predicts a zero normal stress difference)**

**Figure 8**



(a) Streamlines

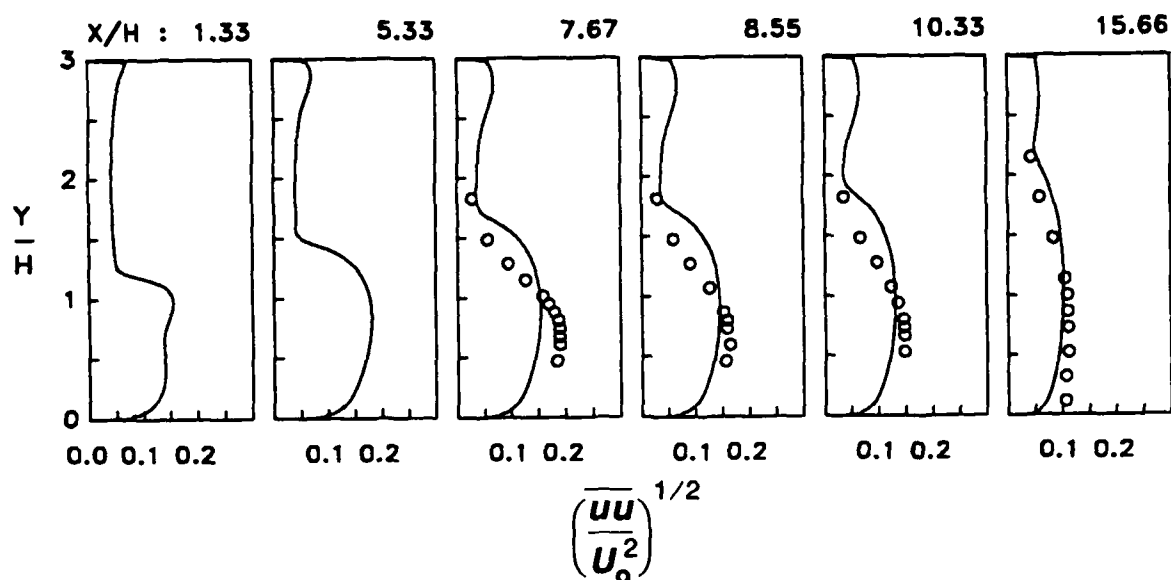


(b) Dimensionless Mean Velocity Profile

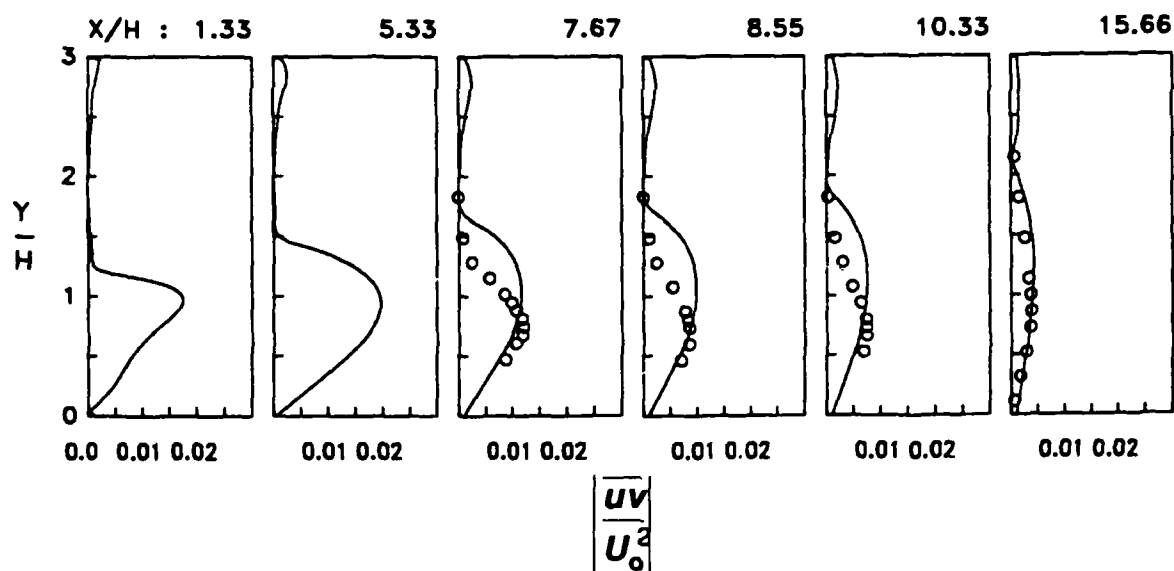
(—— Computations with the three layer model;  
 o Experiments of Kim *et al*, 1980; Eaton & Johnston, 1981)

**Computed Flowfield for the RNG K- $\epsilon$  Model**  
 [E = 1:3; Re = 132,000; 200x100 mesh;  $C_\mu = 0.0837$ ;  $C_{\epsilon 1} = 1.063$ ;  
 $C_{\epsilon 2} = 1.7215$ ;  $\sigma_K = 0.7179$ ;  $\sigma_\epsilon = 0.7179$ ;  $\kappa = 0.372$ ]

Figure 9



(a) Turbulence Intensity



(b) Turbulence Shear Stress

**Computed Turbulence Stresses for the RNG  $K-\epsilon$  Model** [ $E = 1.3$ ;  $Re = 132,000$ ;  $200 \times 100$  mesh;  $C_\mu = 0.0837$ ;  $C_{\epsilon 1} = 1.063$ ;  $C_{\epsilon 2} = 1.7215$ ;  $\sigma_K = 0.7179$ ;  $\sigma_\epsilon = 0.7179$ ;  $\kappa = 0.372$ ; — Computations with the three layer model;  $\circ$  Experiments of Kim *et al*, 1980; Eaton & Johnston, 1981]

Figure 10

# Report Documentation Page

1. Report No. NASA CR-187532 ICASE Report No. 91-23		2. Government Accession No.		3. Recipient's Catalog No.	
4. Title and Subtitle  TURBULENT SEPARATED FLOW PAST A BACKWARD-FACING STEP: A CRITICAL EVALUATION OF TWO-EQUATION TURBULENCE MODELS				5. Report Date February 1991	
				6. Performing Organization Code	
7. Author(s)  S. Thangam C. G. Speziale				8. Performing Organization Report No. 91-23	
				10. Work Unit No. 505-90-52-01	
9. Performing Organization Name and Address Institute for Computer Applications in Science and Engineering Mail Stop 132C, NASA Langley Research Center Hampton, VA 23665-5225				11. Contract or Grant No. NAS1-18605	
				13. Type of Report and Period Covered Contractor Report	
12. Sponsoring Agency Name and Address National Aeronautics and Space Administration Langley Research Center Hampton, VA 23665-5225				14. Sponsoring Agency Code	
15. Supplementary Notes Langley Technical Monitor: Submitted to Physics of Fluids A Michael F. Card					
Final Report					
16. Abstract  The ability of two-equation models to accurately predict separated flows is analyzed from a combined theoretical and computational standpoint. Turbulent flow past a backward facing step is chosen as a test case in an effort to resolve the variety of conflicting results that have been published during the past decade concerning the performance of two-equation models. It is found that the errors in the reported predictions of the K- $\epsilon$ model have two major origins: (1) numerical problems arising from inadequate resolution, and (2) inaccurate predictions for normal Reynolds stress differences arising from the use of an isotropic eddy viscosity. Inadequacies in near wall modeling play a substantially smaller role. Detailed calculations are presented which strongly indicate the standard K- $\epsilon$ model -- when modified with an independently calibrated anisotropic eddy viscosity -- can yield surprisingly good predictions for the backstep problem.					
17. Key Words (Suggested by Author(s))  turbulent separated flow; backward-facing step; K- $\epsilon$ model			18. Distribution Statement  34 - Fluid Mechanics and Heat Transfer  Unclassified - Unlimited		
19. Security Classif. (of this report) Unclassified		20. Security Classif. (of this page) Unclassified		21. No. of pages 27	
				22. Price A03	